Surface Acidity and Basicity of a Rutile Powder

Luca Ferretto and Antonella Glisenti*

Dipartimento di Chimica Inorganica, Metallorganica ed Analitica, Università di Padova, via Loredan, 4, 35131 Padova, Italy

Received July 19, 2002. Revised Manuscript Received January 6, 2003

In this work, the interaction of a rutile powder sample with pyridine, 2,6-lutidine, CO, and CO_2 was studied, at atmospheric pressure and under high-vacuum conditions, to investigate the acid/base character of the surface. The rutile powder has been characterized with DRIFT and XP spectroscopies, XRD, and thermal analysis. The adsorption experiments carried out at atmospheric pressure have been studied by means of DRIFT spectroscopy, whereas QMS and XPS have been used to follow the reactions under HV conditions. The comparison between the obtained results revealed the presence of Lewis acid sites on the TiO_2 rutile surface. At least two nonequivalent Lewis acidic sites have been observed by means of CO chemisorption; basic sites were studied by adsorption of CO_2.

Introduction

The investigation of the reactivity of oxide surfaces is getting more and more important because of their increasing application as catalysts or sensors. Acid and base active surface sites, in particular, can be relevant in determining the interaction mechanisms between the surface and the reagents or products, or between the surface and the reaction intermediates. Moreover, the reaction paths can be deeply influenced by the acidic and basic character of the catalyst.[1]

The aim of this paper is to understand the acid/base character of a rutile powder surface. TiO_2 is frequently used as a support in composite catalysts technology. In particular the system V_2O_5/TiO_2 was deeply investigated;[2−6] and in fact, these catalysts have found industrial application for partial oxidation reactions (*o*-xylene to phthalic anhydride), for the ammoxidation of aromatic hydrocarbons, and in the selective catalytic reduction of nitrogen oxides.[7−19]

Moreover, titania itself may be modified to became a superacid material and it is particularly efficient in several photocatalytic processes.[20]

Several studies concerning the reactivity of anatase with respect to organic molecules,[21−26] as well as papers aiming to understand the surface acid and base properties of anatase[27] and of titania-based mixed oxides[28,29] are present in the literature; some papers are focused on the reactivity of TiO_2 single-crystal surfaces.[30−38] The reactivity of the rutile powder, on the contrary, still needs to be better investigated. Only a few papers concerning the interaction with different molecules give some insights into the acid−base character of the rutile

* Corresponding author. E-mail: glisenti@chin.unipd.it.

(1) Corma, A. *Chem. Rev.* **1995**, *95*, 559.
(2) Busca, G. *Langmuir* **1986**, *2*, 577.
(3) Chary, K. V. R.; Kishan, G.; Bhaskar, T.; Sivaraj, C. *J. Phys. Chem. B* **1988**, *102*, 6792.
(4) Feil, F. S.; van Ommen, J. G.; Ross, J. R. H. *Langmuir* **1987**, *3*, 668.
(5) Busca, G.; Centi, G.; Marchetti, L.; Trifiro, F. *Langmuir* **1986**, *2*, 568.
(6) Vuurman, M. A.; Wachs, I. E.; Hirt, A. M. *J. Phys. Chem.* **1991**, *95*, 5, 9928.
(7) Bond, G. C. *J. Catal.* **1989**, *116*, 531.
(8) Bond, G. C.; Sarkany, J.; Parfitt, G. D. *J. Catal.* **1979**, *57*, 476.
(9) Rylander, P. N. In *Catalysis: Science and Technology*; Anderson, J. R., Boudart, M., Eds.; Springler-Verlag: New York, 1983; Chapter I.
(10) Sanati, M.; Andersson, A. *J. Mol. Catal.* **1990**, *59*, 233.
(11) Sanati, M.; Andersson, A. *J. Mol. Catal.* **1993**, *81*, 51.
(12) Schneider, H.; Tschudin, S.; Schneider, M.; Wokaun, A.; Baiker, A. *J. Catal.* **1994**, *147*, 5.
(13) Kantcheva, M.; Bushev, V.; Klissurski, D. *J. Catal.* **1994**, *145*, 96.
(14) Centi, G.; Nigro, C.; Perathoner, S.; Stella, G. *Catal. Today* **1993**, *17*, 159.
(15) Busca, G. *J. Chem. Soc., Faraday Trans.* **1993**, *89*, 753.
(16) Jonson, B.; Rebenstorf, B.; Larsson, R.; Lars, S.; Andersson, T. *J. Chem. Soc., Faraday Trans.* **1988**, *84*, 3547.
(17) Ramis, G.; Cristiani, C.; Forzatti, P.; Busca, G. *J. Catal.* **1990**, *124*, 574.
(18) Cristiani, C.; Forzatti, P.; Busca, G. *J. Catal.* **1989**, *116*, 586.
(19) Busca, G.; Tittarelli, P.; Tronconi, E.; Forzatti, P. *J. Solid State Chem.* **1987**, *67*, 91.
(20) Linsebigler, A. L.; Lu, G.; Yates, J. T., Jr. *Chem. Rev.* **1995**, *95*, 735.
(21) Suda, Y.; Morimoto, T.; Nagao, M. *Langmuir* **1987**, *3*, 99.
(22) Lavalley, J. C.; Lamotte, J.; Busca, G.; Lorenzelli, V. *J. Chem. Soc., Chem. Commun.* **1985**, 1006.
(23) Hussein, G. A. M.; Sheppard, N.; Zaki, M. I.; Fahim, R. B. *J. Chem. Soc., Faraday Trans.* **1991**, *87*, 2655.
(24) Aas, N.; Pringle, T. J.; Bowker, M. *J. Chem. Soc., Faraday Trans.* **1994**, *90*, 1015.
(25) Rossi, P. F.; Busca, G.; Lorenzelli, V.; Saur, O.; Lavalley, J. C. *Langmuir* **1987**, *3*, 52.
(26) Groff, R. P.; Manogue, W. H. *J. Catal.* **1984**, *87*, 461.
(27) Morterra, C. *J. Chem. Soc., Faraday Trans. 1* **1988**, *84*, 1617.
(28) Lahousse, C.; Aboulayt, A.; Maugé, F.; Bachelier, J.; Lavalley, J. C. *J. Mol. Catal.* **1993**, *84*, 283.
(29) Hino, M.; Arata, K. *Bull. Chem. Soc. Jpn.* **1994**, *67*, 1472.
(30) Kim, K. S.; Barteau, M. A. *Langmuir* **1990**, *6*, 1485.
(31) Idriss, H.; Pierce, K.; Barteau, M. A. *J. Am. Chem. Soc.* **1991**, *113*, 715.
(32) Diebold, U.; Madey, T. E. *J. Vac. Sci. Technol. A* **1992**, *10*, 2327.
(33) Pan, J.-M., Maschhoff, B. L.; Diebold, U.; Madey, T. E. *J. Vac. Sci. Technol. A* **1992**, *10*, 2470.
(34) See, A. K.; Bartynski, R. A. *J. Vac. Sci. Technol. A* **1992**, *10*, 2591.
(35) Lu, G.; Linsebigler, A.; Yates, J. T., Jr. *J. Phys. Chem.* **1994**, *98*, 11733.
(36) Idriss, H.; Lusvardi, V. S.; Barteau, M. A. *Surf. Sci.* **1996**, *348*, 39.
(37) Henderson, M. A. *Surf. Sci.* **1996**, *355*, 151.
(38) Suzuki S.; Yamaguchi Y.; Onishi H.; Sasaki T.; Fukui K.; Iwasawa, Y. *J. Chem. Soc., Faraday Trans.* **1998**, *94*, 161.

10.1021/cm021269f CCC: $25.00
Published on Web 02/08/2003

powder surface;[39,40] moreover, the rutile samples are frequently poorly investigated commercial powders with significant amounts of surface impurities.

Our purpose is to study the acid and base surface sites of a well characterized nano-dimensioned rutile powder (prepared in our laboratory) by means of the adsorption of probe molecules: Lewis and Brönsted acid sites (hereafter L^a_s and B^a_s, respectively) may be present on an oxide surface.[41] Pyridine, 2,6 dimethyl pyridine (lutidine), and CO were selected to test the acid sites, whereas CO_2 was preferred to investigate the basic sites. The adsorption of pyridine was employed by Parry in 1963 to detect the L^a_s and B^a_s on oxide surfaces[42] (IR spectroscopy can readily distinguish pyridine coordinated with L^a_s from the pyridinium ion originated by the interaction between pyridine and B^a_s).[43,44]

Pyridine H-bound to the hydroxyl groups can also be distinguished. Lutidine, because of the steric hindrance, is preferentially adsorbed on the B^a_s whenever the adsorption is perpendicular to the planar surfaces.[45−48] CO, a weak Lewis base, can emphasize the surface acidic sites heterogeneity, as demonstrated by Morterra et al. on several anatase samples.[49] In fact, CO may interact with the surface cationic centers (L^a_s) by means of the C end; this interaction can modify the CO bond order and then the C−O stretching frequency.[50]

Different surface species can result from the CO_2 adsorption according to the acid/base character of the surface.[51−54] The adsorption on an OH group gives rise to the formation of bicarbonate species, whereas the interaction with a L^a_s causes the formation of superficial carbonyl groups. The adsorption on basic sites (coordinatively unsaturated oxygen anions) originates unidentate carbonates, whereas the interaction with an acid metal ion and its neighboring basic oxygen or with two acid metal ions originates a bidentate or bridge carbonate.

The rutile powder was characterized by means of diffuse reflectance infrared Fourier transform (DRIFT) spectroscopy, X-ray photoelectron spectroscopy (XPS), X-ray diffraction (XRD), and thermal analysis (TGA-DSC).

The exposures have been carried out at atmospheric pressure and under high-vacuum (HV) conditions. In the first case the chemisorptions have been studied by means of the DRIFT spectroscopy, and quadrupolar mass spectrometry (QMS) and XPS have been used to follow the reactions under HV conditions. Between the experiment in HV and the one at atmospheric pressure many significant differences are present: the HV experiment is carried out in a strictly controlled atmosphere, while "real-world" conditions are approached in the atmospheric pressure reactor. Moreover, in the HV experiment the reaction chamber works in flow conditions and the contact times between reagents and surface and between products and surface are different from those used in the atmospheric pressure reactor.

It is noteworthy that both the HV experiment and the atmospheric-pressure one were carried out while avoiding any activation or cleaning treatment. The effect of the activation/cleaning procedures on the surface reactivity will be the subject of following papers.

Experimental Section

Sample Preparation. TiO_2 was prepared by precipitation from an acid solution of Ti^{4+} ions. This solution was obtained by dissolving 10 g of titanium sponge in 200 mL of HCl (Sigma-Aldrich, 37%). The solution was treated with HNO_3 (Sigma-Aldrich, 70%) and concentrated H_2SO_4. Titanium hydroxyde was precipitated by adding NH_4OH (Sigma-Aldrich, 28%). The precipitate was filtered and washed with bi-distilled water until pH = 7; then it was dried at 673 K in air for 4 h and calcined at 1173 K in air for 18 h.

Before the HV chemisorption, the sample was processed as a pellet (by pressing the catalyst powder at 2×10^8 Pa for 10 min) and evacuated for 20 min at room temperature (RT) in rough vacuum.

Reaction Conditions. Pyridine and lutidine for the adsorption experiments (Sigma-Aldrich, spectroscopic grade) were used without further purification.

The exposure of the pellet to pyridine and lutidine under HV conditions was carried out at temperatures ranging from RT to 723 K, at a total pressure of ca. 4×10^{-4} Pa. Probe molecules vapors were obtained by evaporation under vacuum; the HV reactor, directly connected to the XPS analysis chamber, allows us to work in flow conditions. Volatile products were characterized by means of a quadrupole gas analyzer (European Spectrometry Systems, ESS). Background gas contributions to the QMS spectrum were eliminated by subtracting from each spectrum recorded after chemisorption the one obtained just before. Mass spectra assignments were made in reference to the fragmentation patterns.[55] Mass data were analyzed by using the method proposed by Ko et al.[56] The temperature of the pellet was evaluated through a thermocouple directly in contact with the sample holder.

Exposure of the powder samples to the probe molecules in the FTIR equipment at atmospheric pressure has been done by using the Spectra-Tech Inc. COLLECTOR apparatus for DRIFT spectroscopy fitted with a high-temperature, high-pressure (HTHP) chamber. For the adsorption of pyridine and lutidine the HTHP chamber was filled with N_2 vapors flowing through a bubbler containing the liquid, but for CO and CO_2 the gas outlet was connected directly to the reaction chamber.

FTIR Measurements. IR spectra were obtained by means of a Brüker IFS 66 spectrometer in the diffuse reflectance mode and displayed in Kubelka−Munk units.[57,58] The resolution of the spectra was 4 cm^{-1}. The sample temperature was measured through a thermocouple inserted into the sample holder directly in contact with the powder.

(39) Primet, M.; Pichat, P.; Msathieu M.-V. *J. Phys. Chem.* **1971**, *75*, 1221.
(40) Hadjiivanov, K. Appl. *Surf. Sci.* **1998**, *135*, 331.
(41) Kung, H. H. *Transition Metal Oxides: Surface Chemistry and Catalysis*; Elsevier: Amsterdam, The Netherlands, 1989; Chapter 5.
(42) Parry, E. P. *J. Catal.* **1963**, *2*, 371.
(43) Morterra, C.; Chiorino, A.; Ghiotti, G.; Garrone, E. *J. Chem. Soc., Faraday Trans. 1* **1979**, *75*, 271.
(44) Nortier, P.; Fourre, P.; Mohammed Saad, A. B.; Saur, O.; Lavalley, J. C. *Appl. Catal.* **1990**, *61*, 141.
(45) Benesi, H. A. *J. Catal.* **1973**, *28*, 176.
(46) Jacobs, P. A.; Heylen, C. P. *J. Catal.* **1974**, *34*, 267.
(47) Matulewicz, E. R. A.; Kerkhof, F. P. J. M.; Moulijn, J. A.; Reitsma, H. J. *J. Colloid Interface Sci.* **1980**, *77*, 110.
(48) Corma, A.; Rodellas, C.; Fornes, V. *J. Catal.* **1984**, *88*, 374.
(49) Morterra, C.; Ghiotti, G.; Garrone, E.; Fisicaro, E. *J. Chem. Soc., Faraday Trans. 1* **1980**, *76*, 2102.
(50) Busca, G. *Catal. Today* **1998**, *41*, 191.
(51) Auroux, A.; Gervasini, A. *J. Phys. Chem.* **1990**, *94*, 6371.
(52) Rethwisch, D. G.; Dumesic, J. A. *Langmuir* **1986**, *2* (1), 73.
(53) Lavalley, J. C. *Trends Phys. Chem.* **1991**, *2*, 305.
(54) Martin, D.; Duprez, D. *J. Mol. Catal. A: Chem.* **1997**, *118*, 113.
(55) Lias, S. G.; Stein, S. E. NIST/EPA/MSDC Mass Spectral Database; PC version 3.0; June, 1990.
(56) Ko, E. I.; Benzinger, J. B.; Madix, R. J. *J. Catal.* **1980**, *62*, 264.
(57) Kubelka, P.; Munk, F. *Z. Tech. Phys.* **1931**, *12*, 593.
(58) Kortum, G. *Reflectance Spectroscopy*; Springer: New York, 1969.

Table 1. XRD Data (Crystallographic Planes Distances in Å) Obtained for the TiO_2 Powder Sample Compared to the JCPDS Cards Data

TiO_2 (this work)	*h k l*	TiO_2 (rutile)[a]
3.246 (100)	1 1 0	3.247 (100)
1.686 (56)	2 1 1	1.687 (60)
2.486 (40)	1 0 1	2.487 (50)
2.186 (25)	1 1 1	2.188 (25)
1.623 (14)	2 2 0	1.623 (20)
1.359 (15)	3 0 1	1.359 (20)
2.053 (8)	2 1 0	2.054 (10)
2.295 (8)	2 0 0	2.297 (8)

[a] Joint Committee on Powder Diffraction Standards card number 21-1276.

XPS Measurements. XP spectra were recorded using a Perkin-Elmer PHI 5600 ci spectrometer with standard Al Kα source (1486.6 eV) working at 350 W. The working pressure was less than 1×10^{-8} Pa. The spectrometer was calibrated by assuming the binding energy (BE) of the Au $4f_{7/2}$ line to be 84.0 eV with respect to the Fermi level. Extended spectra (survey) were collected in the range 0−1350 eV (187.85 eV pass energy, 0.4 eV step, 0.05 s·step^{-1}). Detailed spectra were recorded for the following regions: C 1s, O 1s, Ti 2p (11.75 eV pass energy, 0.1 eV step, 0.1 s·step^{-1}) The standard deviation in the BE values of the XPS line is 0.10 eV. The atomic percentage, after a Shirley type background subtraction,[59] was evaluated using the PHI sensitivity factors.[60] To take into account charging problems the C 1s peak was considered to be located at 285.0 eV and the peaks BE differences were evaluated.

Other Measurements. Thermogravimetric analysis (TGA) and differential scanning calorimetry (DSC) were carried out in a controlled atmosphere using the simultaneous differential techniques (SDT) 2960 of the TA Instruments. Thermograms were recorded at 3 and 10 °C min^{-1} heating rates in air and in N_2. The covered temperature range is from RT to 1273 K.

XRD patterns were obtained with a Philips diffractometer with Bragg−Brentano geometry using Cu Kα radiation (40 kV, 40 mA, $\lambda = 0.154$ nm).

BET surface area measurements were determined using a Carlo Erba Sorptomatic 1900 adsorbing N_2 at its boiling temperature. The sample was previously evacuated for 6 h at 423 K.

Results and Discussion

Sample Characterization. XRD pattern (Table 1) coincides with that of rutile;[61] the crystallite mean diameter (obtained by means of the Scherrer formulas) is 76 nm.[62]

The surface area, determined with the BET method, is 8.34 m^2/g. This rather low value of surface area is frequently observed in the rutile samples (mainly commercial samples).[21,63] In a few cases higher values (around 20−30 m^2/g) are obtained.[40,64,65] This result is a consequence of the high-temperature treatment necessary to obtain pure rutile powder samples.[66]

The XP survey of the rutile powder before adsorption never shows the presence of N or S.

Table 2. Ti 2p3/2 and O 1s XPS Data (eV) for Ti, TiO_2, and Related Compounds, and Binding Energy Differences (ΔBE) between O 1s and Ti 2p3/2 Peaks ($\Delta BE_{(O\ 1s\ -\ Ti\ 2p3/2)}$) and between Ti 2p3/2 and Ti 2p1/2 Peaks, ($\Delta BE_{(Ti\ 2p3/2\ -\ Ti\ 2p1/2)}$)[a]

	Ti 2p3/2	O 1s	ΔBE (Ti 2p3/2 − Ti 2p1/2)	ΔBE (O 1s − Ti 2p3/2)
this work	458.9	530.1 531.7	5.6	71.2
TiO_2 (rutile)	458.5−458.7	530.0	5.6	71.3−71.5
TiO_2 (anatase)	458.5−458.7	530.0	5.2	71.3−71.5
Ti	453.8−454.0		6.2	

[a] NIST Standard Reference Database 20, Version 3.0.

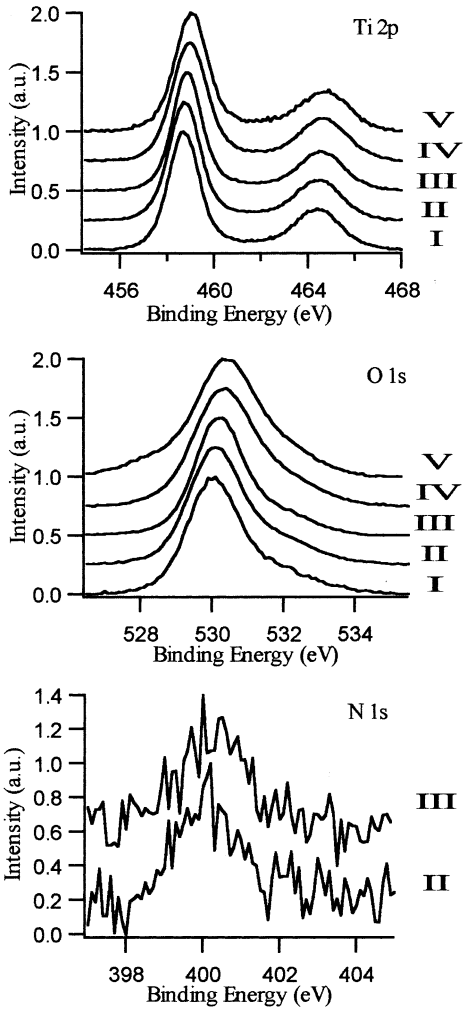

Figure 1. Ti 2p, O 1s, and N 1s XP spectra obtained for the TiO_2 powder (I) before the chemisorptions, (II) after the chemisorption of pyridine at RT, (III) after the chemisorption of pyridine at 473 K, (IV) after the chemisorption of CO_2 at RT, and (V) after the chemisorption of CO_2 at 473 K.

The Ti $2p_{3/2}$ peak lies at 458.9 eV (Table 2 and Figure 1), i.e., in comparable agreement with literature data for Ti(IV) in TiO_2.[67] Furthermore, both the energy position of the O 1s peak (530.1 eV; Figure 1) and the BE difference between O 1s and Ti $2p_{3/2}$ peaks,

(59) Shirley, D. A. *Phys. Rev.* **1972**, *55*, 4709.
(60) Moulder, J. F.; Stickle, W. F.; Sobol, P. E.; Bomben, K. D. In *Handbook of X-ray Photoelectron Spectroscopy*; Chastain, J., Ed.; Physical Electronics: Eden Prairie, MN, 1992.
(61) Joint Committe on Powder Diffraction Standards; card number 21-1276.
(62) Enzo, S.; Polizzi, S.; Benedetti, A. *Z. Kristall.* **1985**, *170*, 275.
(63) Munuera, G. *J. Catal.* **1970**, *18*, 19.
(64) Jones, P.; Hockey, J. A. *Trans. Faraday Soc.* **1971**, *67*, 2669.
(65) Griffiths, D. M.; Rochester, C. H. *J. Chem. Soc., Faraday 1* **1977**, *73*, 1510.

(66) For this reason the TiO_2 powder samples used in catalysis are constituted by anatase or by a mixture of rutile and anatase; the comprehension of the reactivity of titanium oxide based material, however, cannot be reached without a full understanding of the reactivity of rutile.

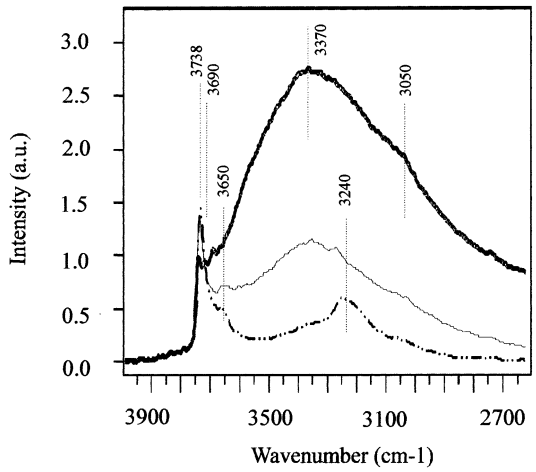

Figure 2. IR spectra obtained for the rutile powder sample at RT (—), at 523 K (—) and at 723 K (—···—···—).

($\Delta BE_{(O\ 1s-Ti\ 2p_{3/2})}$; Table 2) agree with the expected values. The obtained O/Ti atomic ratio is 2.1.

The BE difference between Ti $2p_{3/2}$ and Ti $2p_{1/2}$ peaks, ($\Delta BE_{(Ti\ 2p_{3/2}-Ti\ 2p_{1/2})}$; Table 2), is consistent with the presence of rutile.[68]

The air-exposed surface of TiO_2 is highly hydroxylated, as demonstrated by the asymmetry of the O 1s XPS peak on its higher BE side (Figure 1). The fitting procedure reveals the presence of two contributions around 530.1 and 531.7 eV attributed to Ti−O and to Ti−OH species, respectively.[69]

The IR spectrum (at RT) of the rutile powder in the O−H stretching region (Figure 2), shows the following peaks: 3370 cm^{-1} (with a shoulder around 3050 cm^{-1}) and 3738 cm^{-1}; a weaker contribution is visible around 3690 cm^{-1}. The broad band at ca. 3370 cm^{-1} is ascribed to H-bound water. Consistently, a broad peak due to the bending vibration of water molecules is observed around 1640 cm^{-1}, and suggests the presence of water aggregates.[70] According to this assignment the intensity of the band at 3370 cm^{-1} significantly decreases with increasing temperature (Figure 2). The remaining peaks (3738 and 3690 cm^{-1}) are attributed to the stretching vibrations of isolated and H-bound OH groups.[21,71,72]

The distribution and reactivity of these OH groups strongly depends on the preparation procedure, sample history, and exposed faces.[72]

The temperature increase causes the intensity increment of the peak around 3738 cm^{-1} and the appearance of a new peak at 3650 cm^{-1}; moreover, the decrease of the band at 3370 cm^{-1} allows observation of a new contribution around 3240 cm^{-1} tentatively attributed to the presence of H_2O tightly bound to the rutile powder surface.

On the massive scale, rutile is known to crystallize such that the majority of the external crystal surface is composed by three planes: (110), (101), and (100).[73,74] Figure 3 illustrates the models proposed for the stoichiometric rutile (110), (101), (100) surfaces, respectively. Of these, the first usually has the greatest preponderance. However, the size, shape, and crystallinity of nanoparticles depend on the method of preparation and the particles' dimensions.[75] XRD data collected on our rutile powder sample are also consistent with the presence of (111) surface planes (Table 1). In Figure 3 the model proposed for the (111) surface is illustrated.

The interaction between TiO_2 (110) and H_2O has received considerable attention. Experimental and theoretical data suggest that water interacts mainly molecularly with the TiO_2 surface: structural defects (steps, edges) may play an important role in the dissociation.[76] Undissociated H_2O molecules can H-bind with the OH groups; moreover, a stronger interaction is possible with L^a_s. In the first case water is expected to be removed at lower temperature.[77] These data allow attribution of the broad peak around 3370 cm^{-1} to H_2O H-bound to the OH groups; whereas the peak observed, at higher temperature, at 3240 cm^{-1} can correspond to water molecules bound to L^a_s. The band at 3650 cm^{-1} was assigned to isolated OH groups on the rutile (110) surface, while the peak around 3738 cm^{-1} was attributed by Griffiths et al.[77] to the residual presence of silanol groups; in the present case XPS results allow exclusion of this hypothesis.

It is noteworthy that different OH groups are present on the rutile surfaces: OH groups coordinated to a single octahedral Ti^{4+}, and bridging OH groups which link two or three octahedral cations. The OH stretching frequency usually decreases from the single- to the three-coordinated OH groups,[72] suggesting for the peak at 3738 cm^{-1} a single coordination, and for the peak at 3650 a bi- or tri-fold coordination.

Tsyganenko et al. attributed the two peaks observed around 3670 and 3650 cm^{-1} on an anatase surface to bicoordinated OH groups.[78] In fact, single-coordinated OH groups can form on the O-terminated (110), (100), (101), and (111) surfaces; and bicoordinated OH groups can form on the (111), (100), (101), and (110) Ti-terminated surfaces. Finally, three-coordinated OH groups can be exposed on the (110) Ti-terminated surface (Figure 3).

The behavior of the peaks at 3738 and 3690 cm^{-1} observed as a function of temperature suggests that the IR band due to OH groups perturbed by H-bond with H_2O, shifts from 3738 to 3690 cm^{-1}.

Finnie et al.[79] observed, on a nanocrystalline TiO_2 film, a similar behavior of the OH groups coordinated

(67) NIST XPS Standard Reference Database 20, Version 3.0.
(68) The BE difference between Ti2p3/2 and Ti2p1/2 peaks is expected to be 5.2 eV in anatasia and 6.2 eV in metallic titanium.
(69) McIntyre, N. S.; Chan, T. C. In *Practical Surface Analysis*, 2nd edition. Briggs, D., Seah, M. P., Eds.; John Wiley and Sons: New York, 1990; Vol. 1, Chapter 10.
(70) Yates, D. J. C. *J. Chem. Soc., Faraday Trans. 1* **1961**, *65*, 746.
(71) Little, L. H. *Infrared Spectra of Adsorbed Species*; Academic Press: San Diego, CA, 1966.
(72) Boehm, H. P.; Knözinger, H. In *Catalysis: Science and Technology*. Anderson, J. R., Boudart, M., Eds.; Springer-Verlag: New York, 1983; Vol. 4, Chapter 2.
(73) Jones, P.; Hockey, J. A. *Trans. Faraday Soc.* **1971**, *67*, 2679.
(74) Heinrich, V. E.; Cox, P. A. *The Surface Science of Metal Oxides*; Cambridge University Press: Cambridge, U.K., 1994.
(75) Shklover, V.; Nazeeruddin, M.-K.; Zakeeruddin, S. M.; Barbé, C.; Kay, A.; Haibach, T.; Steurer, W.; Hermann, R.; Nissen, H.-U.; Grätzel, M. *Chem. Mater.* **1997**, *9*, 430.
(76) Stefanovich, E. V.; Truong, T. N. *Chem. Phys. Lett.* **1999**, *299*, 623.
(77) Griffiths, D. M.; Rochester, C. H. *J. Chem. Soc., Faraday Trans. 1* **1977**, *73*, 1510.
(78) Tsyganenko, A. A.; Filimonov, V. N. *J. Mol. Struct.* **1973**, *19*, 579.

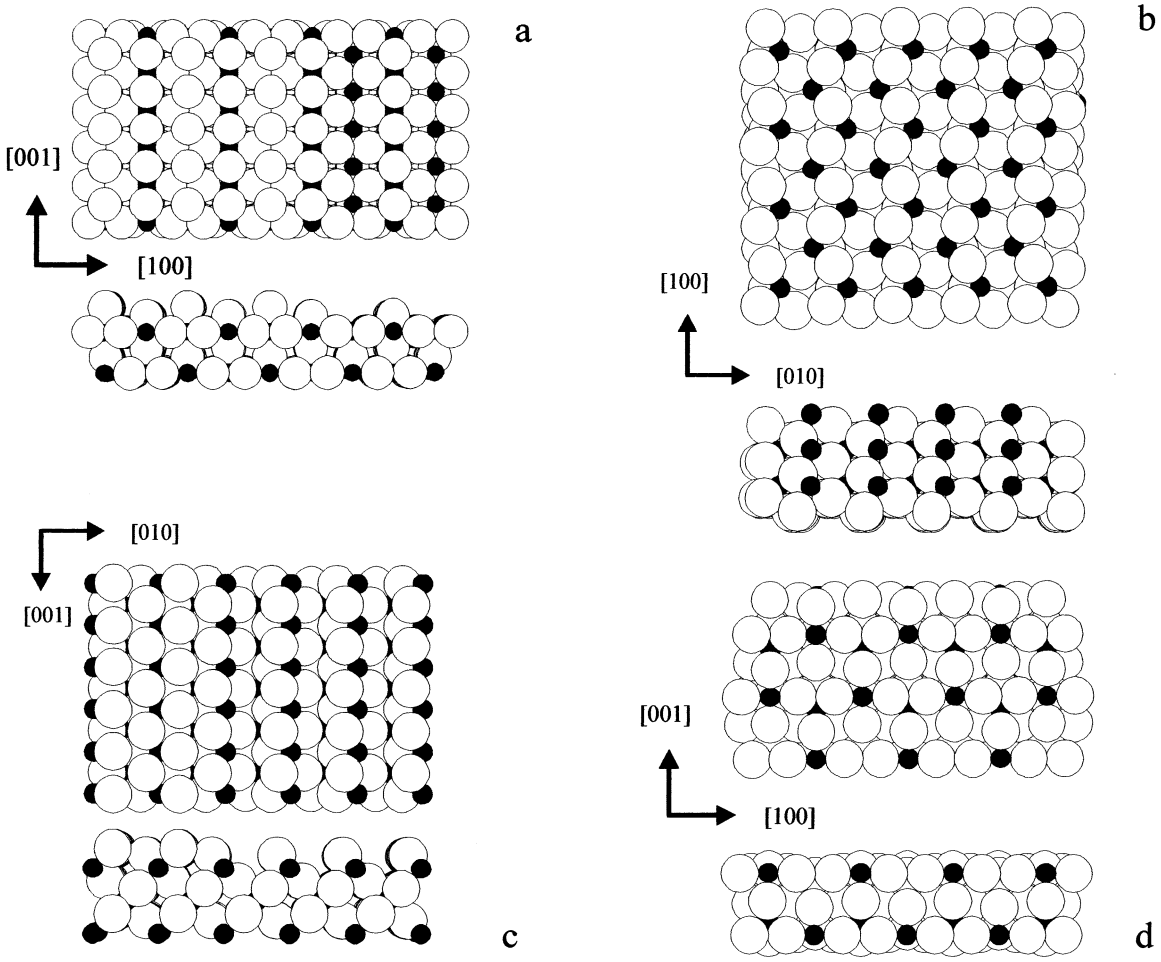

Figure 3. Schematic representation of the exposed rutile faces. (a) (110): O-terminated (left side) and Ti-terminated (right side); (b) (101); (c) (100): O-terminated (left side) and Ti-terminated (right side); (d) (111). Large spheres, O; small spheres, Ti; top and side views.

Table 3. IR Data (cm^{-1}) Obtained after Exposure of the Rutile Powder to Pyridine and Reference Data Concerning Pyridine

	Py/ TiO_2 (this work)	pyridine[a]
8a	1606	1583 (vs)
8b	1573	1572 (m)
19a	1487	1482 (s)
19b	1448	1441 (vs)
overtones	1593	1599 (s)

[a] Corrsin, L.; Fax, B. J.; Lord, R. C. *J. Chem. Phys.* **1953**, *21*, 1170.

to a single Ti^{4+} cation, whereas bridging OH groups resulted in unperturbed by H-bonds. Griffith et al., in contrast, suggested that the bridging OH H-bind water molecules: as a consequence the peak around 3650 cm^{-1} shifts to 3520 cm^{-1}.[77]

Reaction with Pyridine. The IR spectrum of rutile powder exposed at RT to a pyridine + N_2 mixture (Figure 4) is characterized by the presence of several peaks at 1606, 1573, 1487, and 1448 cm^{-1} ascribed to the 8a, 8b, 19a, and 19b vibrations of pyridine. The positions and shapes of these peaks agree (Table 3) with the presence of pyridine interacting with the L^a_s (hereafter py-L^a_s).[49,50,80−82]

A small peak around 1593 cm^{-1} is attributed to pyridine H-bound (hereafter H-py) to the surface.

The absence of higher wavenumbers contributions to the peaks due to the vibrations modes 8 and 19, allows exclusion of the formation of pyridinium ions and thus the existence of B^a_s of significant strength on the rutile surface.[50,81]

Moving to the O−H stretching region observed after exposure to pyridine at RT, two peaks at 3720 and 3735 cm^{-1} suggest the formation of isolated OH groups as a consequence of the adsorption of pyridine.

The IR spectrum obtained after the rutile powder exposure to a pyridine + N_2 mixture and then to N_2 (10 min) is shown in Figure 4a. The spectrum inspection indicates that pyridine is strongly bound to the surface L^a_s and is not removed by N_2.

The behavior observed as a function of temperature confirms the high strength of the py-L^a_s bond. The IR data obtained after heating, at increasing temperatures, the rutile powder exposed to pyridine at RT, are shown in Figure 4b; the intensity of the py-L^a_s (1606 and 1448 cm^{-1}) and H-py (1595 cm^{-1}) peaks, as well as the intensity of the peaks attributed to the OH groups

(79) Finnie, K. S.; Cassidy, D. J.; Bartlett, J. R.; Woolfrey, J. L. *Langmuir* **2001**, *17*, 816.
(80) Lahousse, C.; Maugé, F.; Bachelier, J.; Lavalley, J. C. *J. Chem. Soc., Faraday Trans.* **1995**, *91*, 2907.
(81) Miyata, H.; Nakagawa, Y.; Ono, T.; Kobokawa, Y. *J. Chem. Soc., Faraday Trans. 1* **1983**, *79*, 2343.
(82) Tanabe, K. In *Catalysis − Science and Technology*. Anderson, J. R., Boudart, M., Eds.; Springer-Verlag: New York, 1981; Chapter 5.

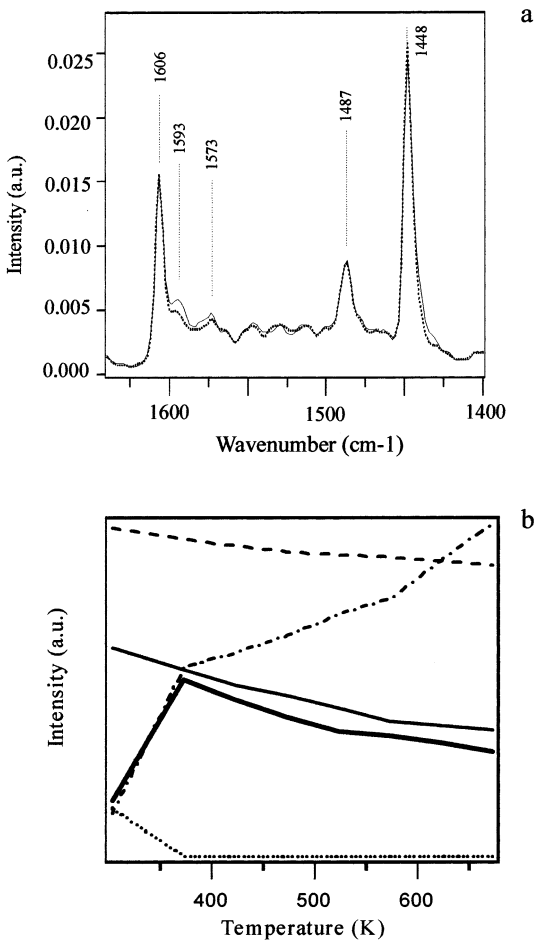

Figure 4. (a) IR spectra obtained after exposure of the rutile powder to a pyridine + N_2 mixture at RT (—), and then to a N_2 flux for 10 min at RT (·····); (b) IR peaks intensities obtained, as a function of temperature, for the rutile powder exposed to a pyridine + N_2 mixture at RT; pyridine bound to Lewis acid sites (– –) 1606 cm^{-1} and (- - -) 1448 cm^{-1}; H-bound pyridine (·····) 1593 cm^{-1}; hydroxyl groups O–H stretching vibrations (·–·–·–) 3735 cm^{-1} and (—) 3720 cm^{-1}.

stretching vibrations (3735 and 3720 cm^{-1}), are shown as a function of temperature.

In fact, the heat treatment until 673 K does not induce the complete desorption of the py-L^a_s.

H-py, on the contrary, completely disappears at 373 K.

The heat treatment at 373 K causes the intensity increase of the two OH stretching peaks, whereas at higher temperatures the intensity of the peak at 3735 cm^{-1} increases and the peak at 3720 cm^{-1} decreases. As a whole, these data suggest that pyridine interacts with the OH groups distributed on the rutile powder surface by means of H-bonds. It is noteworthy that Kazansky et al.[83–85] observed a shift from 3749 to 3722 cm^{-1} as a consequence of the interaction between isolated silanol groups and molecules of low H-bond acceptor strength.

The intensity decrease of the peak at 3720 cm^{-1} is consistent with a condensation mechanism of the surface OH groups and with the temperature-induced desorption of weakly bound pyridine.

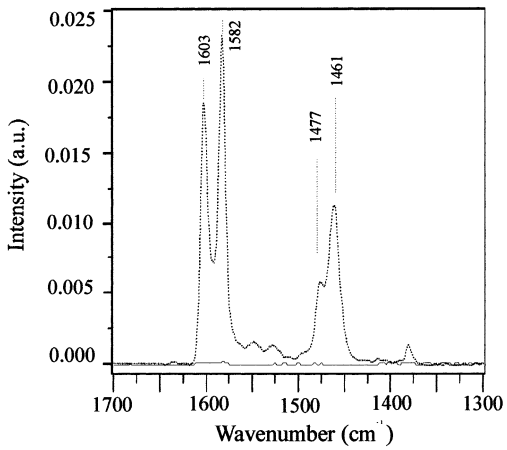

Figure 5. IR spectra obtained after exposure of the rutile powder sample to a lutidine + N_2 mixture at RT (·····), and then to N_2 for 10 min at RT (–).

Table 4. IR Data (cm^{-1}) Obtained on the Rutile Powder Sample after Exposure to 2,6-Lutidine (at RT), and Reference Data Concerning 2,6-Lutidine

	L/TiO_2	lutidine[a]
8a	1603	1590
8b	1582	1582
19a	1477	1470
19b	1461	1460

[a] Bohon, R. L.; Isaac, R.; Hoftiezer, H.; Zellner, R. J. *Anal. Chem.* **1958**, *30*, 245.

The exposure to pyridine was also carried out under HV conditions and followed by means of XPS and QMS. The XP Ti 2p and O 1s peak positions and shapes, and the atomic composition, do not change as a consequence of the chemisorption (Figure 1) suggesting that the interaction with pyridine does not modify the surface.

It is noteworthy that the XPS analysis reveals the presence of nitrogen on the rutile powder surface exposed to pyridine at temperatures increasing from RT to 473 K (Figure 1); XPS results as a whole confirm the strong interaction between pyridine and rutile. The N 1s peak position (400.0 eV) agrees with the expected value for py-L^a_s; moreover, the inspection of the XP N 1s spectrum confirms the absence of pyridinium species.[67] The XPS quantitative analysis reveals the presence of 1% at. of nitrogen chemisorbed on the rutile surface. QMS results never show, at temperatures lower than 473 K, the formation of species due to the oxidation or decomposition of pyridine.

Reaction with 2,6-Lutidine. The IR spectrum obtained after exposure to a lutidine + N_2 mixture at RT (Figure 5) reveals several peaks at 1603, 1582, 1477, and 1461 cm^{-1} (Table 4); the peaks at 1603, 1477, and 1461 cm^{-1} agree with the presence of lutidine very weakly bound to the rutile powder surface.[28,80,82]

The IR spectrum obtained after exposure to N_2 for 10 min (Figure 5), shows the complete absence of lutidine (and confirms its weak interaction with the rutile powder surface). The absence of peaks due to protonated species (around 1625 and 1640 cm^{-1}, as an example) suggests the absence of exposed B^a_s on the rutile powder surface. It is noteworthy that Lahousse et al.[28] obtained on an anatase sample a different result, confirming thus

(83) Kazansky, V. B. *Proc. Int. Congr. Catal. 6th (London 1976)* **1977**, *1*, 50.
(84) Kazansky, V. B.; Gritskov, A. M.; Adreev, V. M.; Zhidomirov, G. M. *J. Mol. Catal.* **1978**, *4*, 135.
(85) Kazansky, V. B. *Zh. Khim. Fiz.* **1982**, *56*, 318.

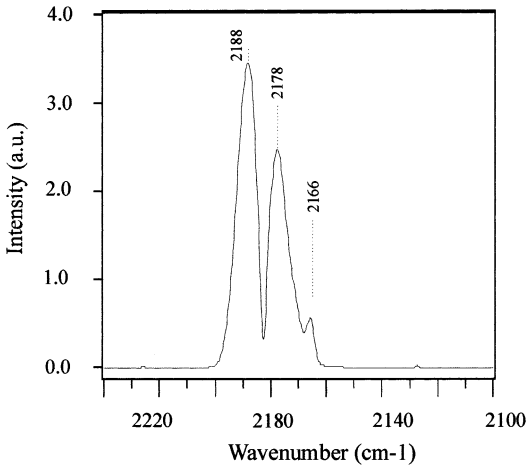

Figure 6. IR spectrum obtained after exposure of the rutile powder to CO at 143 K.

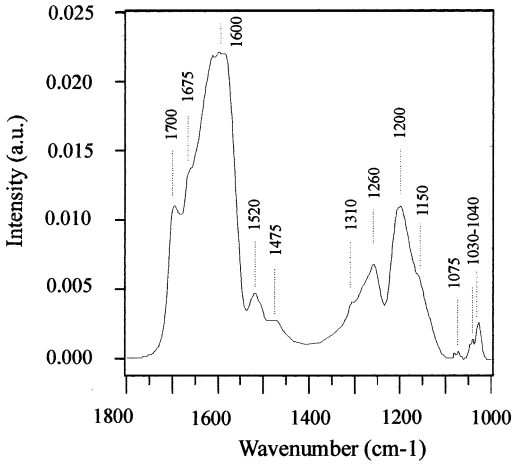

Figure 7. IR spectrum obtained after exposure of the rutile powder sample to CO_2 at RT.

that the acid/base sites distribution strongly depends on the preparation procedure and heat treatments.

Reaction with Carbon Monoxide and Carbon Dioxide. The IR spectrum of rutile powder sample exposed at ca. 143 K to CO, is shown in Figure 6. The spectrum inspection reveals the presence of three peaks centered at 2166, 2178, and 2188 cm^{-1} attributed to the interaction between CO and L^a_s.

The CO stretching frequency shifts toward higher values (gas-phase CO = 2143 cm^{-1}) after interaction with the rutile powder surface (blue-shift) in agreement with the results obtained by Hadjiivanv et al.[86] on anatase and by several authors on rutile,[87] and with the theoretical value calculated by Casarin et al.[88] for the (110) surface of rutile.

The values obtained for the shift of the CO stretching vibration (23, 35, and 45 cm^{-1}, respectively) agree with the presence of medium and high strength acid sites.

Hadjiivanv et al.[86] evidenced the considerable surface heterogeneity of anatase; the exposure to CO at low-temperature results in at least four CO adsorption forms corresponding to the presence of three types of L^a_s (α = 2210 cm^{-1}, β = 2191−2179 cm^{-1}, and γ = 2165 cm^{-1}).

These L^a_s are identified to be four α, and five β and γ, coordinated Ti^{4+} cations exposed on the different crystal planes as well as on some edges. In particular, β-L^a_s are pentacoordinated Ti^{4+} cations bound to three-coordinated O^{2-} anions, while γ-L^a_s are pentacoordinated Ti^{4+} cations bound to bi-coordinated O^{2-} anions.[86] According to literature data, the L^a_s observed on the rutile surface are five-coordinated Ti^{4+} cations. As already observed, rutile exhibits predominantly (110) faces, although (101) and (100) are also common. The β sites can be observed on the (110), (101), and (100) crystal faces (Figure 3).[73] The interaction among CO and five-coordinated Ti^{4+} cations gives rise to the peaks centered around 2178−2188 cm^{-1}. The peak corresponding to the interaction between CO and β-L^a_s shifts to higher frequencies with decreasing coverage.[86]

The interaction with γ-L^a_s causes the CO stretching frequency to shift from 2143 to 2165 cm^{-1}. γ-L^a_s can be observed on the (111) rutile face (Figure 3d). The absence of a signal around 2155 cm^{-1} attributed to the CO H-bound to the surface OH groups confirms the absence of Brönsted acid sites of significant strength. Ti^{3+} L^a_s or tetracoordinated Ti^{4+} were never observed.

The IR spectrum of the rutile powder sample exposed to CO_2 is shown in Figure 7. The spectrum inspection reveals the presence of several peaks, centered around 1600−1700, 1520, 1475, 1200−1260, 1075, and 1030−1040 cm^{-1}. The peaks positions and shapes agree (Table 5) with the formation of different carbonate species as a consequence of the interaction between CO_2 and the rutile powder surface. In particular, the contributions at 1675, 1310, and 1030−1040 cm^{-1} are attributed to bicarbonate species, whereas the weak signal around 1475 cm^{-1} agrees with the presence of unidentate carbonate species.[89] Bicarbonate species form as a consequence of the interaction between CO_2 and OH groups, whereas unidentate carbonates (weak contribution) suggest the presence of basic oxygen sites. The signals at higher wavenumber (1600, 1700 cm^{-1}), as well as the broad contribution around 1150−1220 cm^{-1} and the weak peak at 1520 cm^{-1}, suggest the formation of bidentate species[71,90] and thus the interaction with Ti^{4+} L^a_s and the neighboring oxygen or with two Ti^{4+} L^a_s. Markovits at al.[91] indicate that the interaction with a basic oxygen on the bare rutile surface is not favorable because this surface is too acidic; in contrast, the adsorption on the Ti^{4+} L^a_s is easier. Moreover, on a hydrated surface, the presence of OH groups favors the CO_2 chemisorption and leads to the formation of adsorbed bicarbonate ions from which bidentate carbonate species can form.

Significant TPD results were obtained by Raupp et al.[92] on a polycrystalline titania surface prepared and studied under HV: the desorption patterns allowed the

(86) Hadjiivanov, K.; Lamotte, J.; Lavalley, J.-C. *Langmuir* **1997**, *13*, 3374.
(87) Hadjiivanov, K.; Davidov, A.; Klissurski, D. *Kinet. Katal.* **1988**, *29*, 161. Busca, G.; Saussey, A.; Saur, D.; Lavalley, J. C.; Lorenzelli, V. *Appl. Catal.* **1985**, *14*, 245. Morterra, C.; Garrone, E.; Bolis, V.; Fubini, B. *Spectrochim. Acta, Part A* **1987**, *43*, 1577.
(88) Casarin, M.; Maccato, C.; Vittadini, A. *J. Phys. Chem. B* **1998**, *102*, 10745.
(89) Gatehouse, B. M.; Livingstone, S. E.; Nyholm, R. S. *J. Chem. Soc.* **1958**, 3137.
(90) Reference 66, Chapter 3.
(91) Markovits, A.; Fahmi, A.; Minot, C. *J. Mol. Struct. (THEOCHEM)* **1996**, *371*, 219.
(92) Raupp, G. B.; Dumestic, J. A. *J. Phys. Chem.* **1985**, *89*, 5240.

Table 5. IR Data (Wavenumbers, cm^{-1}) Concerning Carbonate and Bicarbonate Species

	monodentate carbonates[a]	bidentate carbonates[a]	bridging carbonates[a]	bicarbonate[a]
C═O stretching		1577−1493	1870−1750	1660−1655 1630−1620
asymm. C−O stretching	1420−1470	1338−1260	1280−1252	1410−1400 1370−1290
symm. C−O stretching		1082−1055 1050−1021	1021−969	1050−1010 1000−990

[a] Ref. 89. Gatehouse, B. M.; Livingstone, S. E.; Nyholm, R. S. *J. Chem. Soc., Faraday Trans.* **1958**, 3137.

authors to individuate the presence, after exposure to CO_2, of mono e bidentate carbonate species similar to those suggested by our IR data.

The exposure to CO_2 was also carried out under HV and followed by means of XPS and QMS. Ti 2p and O 1s XPS peak positions and shapes, as well as the XPS atomic composition, do not change after the adsorption (Figure 1).

Conclusions

In this work a rutile powder was prepared by precipitation from an acid solution of Ti^{4+} ions. Singly coordinated and bridging OH groups are present on the sample surface and may H-bind H_2O molecules.

The reactivity of the rutile powder with respect to pyridine, lutidine, CO, and CO_2 was investigated.

Pyridine strongly interacts with the rutile powder sample, suggesting the presence of Lewis acid sites.

The weak interaction between lutidine and the rutile powder surface confirms the absence of exposed Brönsted acid sites easy accessible to the sterically hindered lutidine.

The CO chemisorption reveals the presence of β (five-coordinated Ti^{4+} cations bound to three-coordinated O^{2-} anions) and γ (five-coordinated Ti^{4+} cations bound to two-coordinated O^{2-} anions) Lewis acid sites.

CO_2 reacts with the rutile powder with the formation of bicarbonate, uni-, and bi-dentate carbonate species. Unidentate carbonate formation agrees with the existence of basic sites. The presence of bicarbonate and bidentate carbonate species, however, suggests the interaction of CO_2 with a Ti^{4+} L^a_s and the neighboring oxygen or OH groups.

The evacuation of the reaction chamber by means of nitrogen and the thermal treatments at 373 and 473 K allowed investigation of the strength of the acidic and basic sites.

Exposure of the rutile sample to pyridine under HV conditions reveals the interaction between pyridine and surface, confirming the high strength of the Lewis acid sites. It is noteworthy that the interaction with the adsorbed molecules never modified the rutile powder surface. The interaction with CO_2 under HV conditions never revealed the formation of carbonate or bicarbonate species, suggesting that the basic sites on the rutile surface (and then the bond with CO_2) are too weak to withstand the vacuum conditions or that the basic sites are destroyed by the HV. QMS results showed that the oxide surface never decomposed the chemisorbed molecules, confirming their possible validity as acid/base sites test molecules.

A preliminary identification of the acid/base surface sites was attempted by comparing the experimental results with the models of the prevalently exposed surfaces. As a matter of fact, the crystal size and shape of nanoparticles strongly depend on the method of preparation and can deeply influence the powder reactivity. Further work is underway in our laboratory to better investigate the real shape and dimension of the crystallites.[93]

Acknowledgment. We thank Eugenio Tondello for helpful discussions and suggestions during this work; and we also thank Paolo Colombo for the XRD spectra and Loretta Storaro for the surface area measurements.

CM021269F

(93) Transmission electron microscopy (TEM) should allow a better comprehension of the real shape and dimension of the crystallites. As a matter of fact, XRD furnishes a mean particle diameter, and crystallites of lower dimension cannot be adequately investigated. It has to be considered that nanoparticles can show a really interesting reactivity. Moreover, the real shape of the crystallite can be relevant for reactivity: the different exposed crystal faces and the presence of the surface defects (steps, edges) can deeply influence the surface reactivity.